Biosensors and Bioelectronics 54 (2014) 528–533

Contents lists available at ScienceDirect

Biosensors and Bioelectronics

journal homepage: www.elsevier.com/locate/bios

Facile synthesis of tetragonal columnar-shaped TiO_2 nanorods for the construction of sensitive electrochemical glucose biosensor

Zhanjun Yang *, Yan Tang, Juan Li, Yongcai Zhang, Xiaoya Hu *

College of Chemistry and Chemical Engineering, Yangzhou University, Yangzhou 225002, PR China

ARTICLE INFO

Article history:
Received 24 August 2013
Received in revised form
28 October 2013
Accepted 12 November 2013
Available online 23 November 2013

Keywords:
TiO_2 nanorods
Semiconductor material
Glucose oxidase
Direct electrochemistry
Glucose
Biosensor

ABSTRACT

A tetragonal columnar-shaped TiO_2 (TCS-TiO_2) nanorods are synthesized via a facile route for the immobilization of glucose oxidase (GOx). A novel electrochemical glucose biosensor is constructed based on the direct electrochemistry of GOx at TCS-TiO_2 modified glassy carbon electrode. The fabricated biosensor is characterized by scanning electron microscopy, Fourier transform infrared spectroscopy, electrochemical impedance spectra and cyclic voltammetry. The immobilized enzyme molecules on TCS-TiO_2 nanorods retain its native structure and bioactivity and show a surface controlled, quasi-reversible and fast electron transfer process. The TCS-TiO_2 nanorods have large surface area and provide a favorable microenvironment for enhancing the electron transfer between enzyme and electrode surface. The constructed glucose biosensor shows wide linear range from 5.0×10^{-6} to 1.32×10^{-3} M with a high sensitivity of 23.2 mA M^{-1} cm^{-2}. The detection limit is calculated to be 2.0×10^{-6} M at signal-to-noise of 3. The proposed glucose biosensor also exhibits excellent selectivity, good reproducibility, and acceptable operational stability. Furthermore, the biosensor can be successfully applied in the detection of glucose in serum sample at the applied potential of −0.50 V. The TCS-TiO_2 nanorods provide an efficient and promising platform for the immobilization of proteins and development of excellent biosensors.

1. Introduction

The fast and reliable determination of blood glucose levels is of considerable importance for diagnosis and therapy of diabetics (Mizutani and Yabuki, 1997; Liu and Ju, 2003). As an ideal mode enzyme, glucose oxidase (GOx) has been extensively used in fabrication of electrochemical glucose biosensors due to its catalytic ability to oxidize glucose (Vamvakai et al., 2006; Zhao and Ju, 2006; Xu et al., 2010; Jiang et al., 2012b, Li et al., 2013). The ultimate goal of glucose detection is to develop the third generation biosensor based on the direct electron transfer (DET) between the cofactor FAD of GOx and electrode surface without the mediator (Wang, 2008). Unfortunately, the redox center in biomolecules is usually seated deeply in cavity of enzyme molecules, which make it hard to realize DET of enzyme at conventional electrodes (Meng et al., 2009). Over the past few decades, various kinds of nanomaterials, such as gold nanoparticles (Jia et al., 2008; Pingarron et al., 2008), carbon nanotubes (Azamian et al., 2002; Wang and Musameh, 2003; Ammam and Fransaer, 2012), graphene (Kang et al., 2009; Shan et al., 2010a), titanium oxide (Bao et al., 2008) and tin disulfide (Yang et al., 2011) have been explored to immobilize GOx for accelerating DET of redox enzyme on the electrode surface.

TiO_2, a cheap, nontoxic and chemically stable semiconductor with a band gap energy of 3.2 eV, has attracted considerable interest in various areas such as pigment, cosmetic, catalyst, photovoltaic materials and sensors (Koo et al., 2006; Wang et al., 2008; Liang and Li, 2009; Zhang et al., 2009). One-dimensional (1D) TiO_2 nanostructures, especially nanorods, nanowires and nanotubes, are superior to their spherical and planar counterparts due to their high surface-to-volume ratio, increased number of delocalized carriers, and improved charge transport afforded by their dimensional anisotropy (Koo et al., 2006; Wang et al., 2008). To date, 1D TiO_2 nanomaterials have been synthesized by the hydrothermal method (Tian et al., 2008), controlled hydrolysis (Zhang et al., 2009), dissolution-reprecipitation process (Wang et al., 2008), sol–gel process (Koo et al., 2006; Liang and Li, 2009; Attar et al., 2009) and surfactant-templated synthesis (Chung et al., 2006). Here, we reported a facile method for the large scale preparation of tetragonal columnar-shaped TiO_2 (TCS-TiO_2) nanorods by heating a mixture of Ti and NH_4Cl powders in air at a relatively low temperature. To the best of our knowledge, TCS-TiO_2 nanorods have not yet been used to immobilize proteins for the fabrication of biosensor.

Chitosan, a natural biopolymer with unique structure features, is commonly used to disperse nanomaterials and immobilize

* Corresponding authors. Tel./fax: +86 514 87972034.
E-mail addresses: zjyang@yzu.edu.cn (Z. Yang), xyhu@yzu.edu.cn (X. Hu).

0956-5663/$ - see front matter © 2013 Elsevier B.V. All rights reserved.
http://dx.doi.org/10.1016/j.bios.2013.11.043

enzymes for constructing biosensors due to its excellent capability for film formation, nontoxicity, biocompatibility, mechanical strength, good water permeability (Kang et al., 2009). In this work, a facile route was proposed for the preparation of TCS-TiO_2 nanorods from Ti and NH_4Cl powders in air at 400 °C for 3 h. The resulting TCS-TiO_2 nanorods were dispersed with chitosan solution, and for the first time used to modify the electrode for the immobilization of enzyme molecules. Based on DET of GOx at TCS-TiO_2/chitosan modified electrode, a novel electrochemical biosensor was proposed for sensitive detection of glucose. The TCS-TiO_2 enhanced the electron transfer between the enzyme molecules and electrode surface. A pair of obvious and well-defined redox peaks of GOx could be observed at GOx/TCS-TiO_2/chitosan modified electrode. UV–vis and Fourier transform infrared spectrum demonstrated that the TCS-TiO_2/chitosan film provided a favorable microenvironment for GOx to retain its native structure and bioactivity. The constructed biosensor showed high sensitivity, excellent selectivity, good reproducibility and could be successfully applied in reagentless glucose detection. Moreover, the TCS-TiO_2 nanorods provide a potential electrode material for electrochemical biosensing.

2. Materials and methods

2.1. Materials and Reagents

GOx (EC 1.1.3.4, 108 U mg^{-1}, from *Aspergillus niger*) was supplied by Amresco. D-(+)-Glucose and chitosan were purchased from Sigma-Aldrich. Ti and NH_4Cl powders were purchased from Sinopharm Chemical Reagent Co., Ltd. A stock solution of D-glucose was prepared and allowed to mutarotate at room temperature for 24 h prior to use. Phosphate buffer solution (PBS) was a mixture of 0.1 M Na_2HPO_4 and NaH_2PO_4 and its pH was adjusted with H_3PO_4 or NaOH solutions. All other chemicals and reagents are of analytical grade and were prepared using distilled water.

2.2. Apparatus

Electrochemical measurements were carried out on a CHI 852C electrochemical workstation (Co., CHI, Shanghai Chenhua, China). All experiments were performed with a three-electrode system using a glassy carbon electrode (GCE, $D=3$ mm) as the working electrode, a platinum wire as the auxiliary electrode and a saturated calomel electrode (SCE) as reference electrode. The cyclic voltammetric experiments were carried out at a scan rate of 100 mV s^{-1} in an electrochemical cell filled with 5.0 ml of PBS. All pH measurements were performed with S-25 digital pH-meter with glass combination electrode. Scanning electron micrographs (SEM) were obtained with a Hitachi S-4800 scanning electron microscope (Japan) at an acceleration voltage of 15 kV. Fourier transform infrared (FTIR) spectra were measured with a Tensor 27 spectrometer (Bruker Co., Germany). Electrochemical impedance spectroscopy (EIS) measurements were performed on an Autolab/PGSTAT30 (The Netherlands) in 0.1 M KCl solution containing 5 mM $K_3[Fe(CN)_6]/K_4[Fe(CN)_6]$, and the amplitude of the applied sine wave potential was 5 mV. The impedance measurements were recorded at a bias potential of 190 mV within the frequency range from 0.05 Hz to 10 kHz.

2.3. Preparation of TCS-TiO_2 nanorods and enzyme electrodes

Ti (0.02 mol) and NH_4Cl (0.05 mol) powders were mixed and ground homogeneously in a carnelian mortar, then transferred to corundum crucible. The open crucible was heated in a muffle furnace at 400 °C for 3 h, and then allowed to cool at room temperature. The resulting solid powders were collected directly as the final product. 1.0 mg of the as-prepared TCS-TiO_2 was dispersed in 1.0 ml 0.5 wt% chitosan solution with ultrasonication for 30 min. 8.0 mg of GOx was added in the suspension of TCS-TiO_2/chitosan, and homogeneously mixed under gentle stirring for 20 min for the following use.

The GCE was firstly polished successively with 0.03 and 0.05 μm alumina slurry (Buhler) followed by rinsing thoroughly with distilled water, and then sonicated in 1:1 nitric acid–water (v/v), acetone and distilled water and finally dried in air. After 5.0 μl of the resultant suspension was dropped on the surface of the pretreated GCE and dried in silica gel desiccators, the GOx/TCS-TiO_2/chitosan modified electrode was finally obtained. The fabricated enzyme electrode was rinsed thoroughly with distilled water to wash away the loosely adsorbed enzyme molecules. When not in use, the enzyme electrodes were stored at 4 °C in a refrigerator.

3. Results and discussion

3.1. Characterizations of GOx/TCS-TiO_2/chitosan modified electrode

Fig. 1A showed the SEM image of the synthesized TCS-TiO_2 nanorods, and a tetragonal columnar-shaped morphology could be clearly observed. When TCS-TiO_2 nanorods were dispersed in chitosan solution, the SEM image of the TCS-TiO_2/chitosan was shown in Fig. 1B. It could be seen that TCS-TiO_2 displayed a uniform and ordered arrays structure, which was suitable platform for the immobilization of GOx and fabrication of functional biosensor for glucose. After GOx molecules were trapped in the TCS-TiO_2/chitosan composite, its SEM (Fig. 1C) exhibited obviously different surface morphology from the TCS-TiO_2/chitosan. The aggregates of the loaded enzymes were distributed regularly and

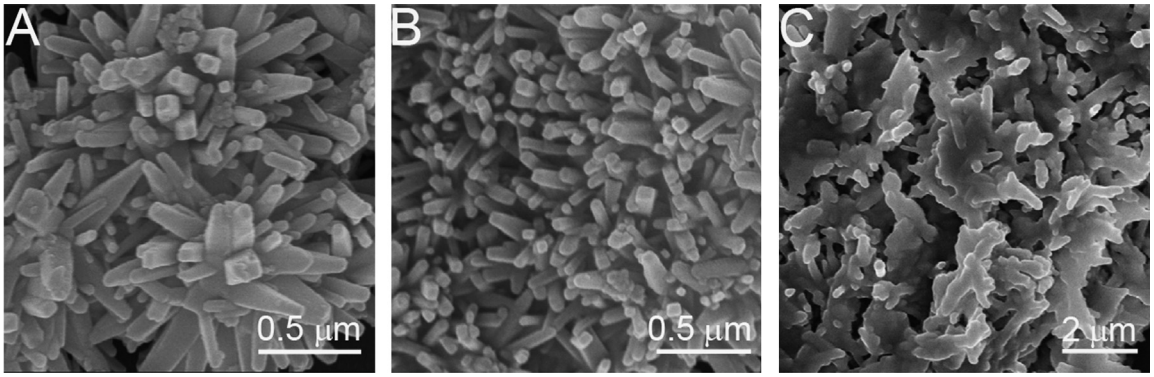

Fig. 1. SEM images of TCS-TiO_2 (A), TCS-TiO_2/chitosan (B) and GOx/TCS-TiO_2/chitosan (C).

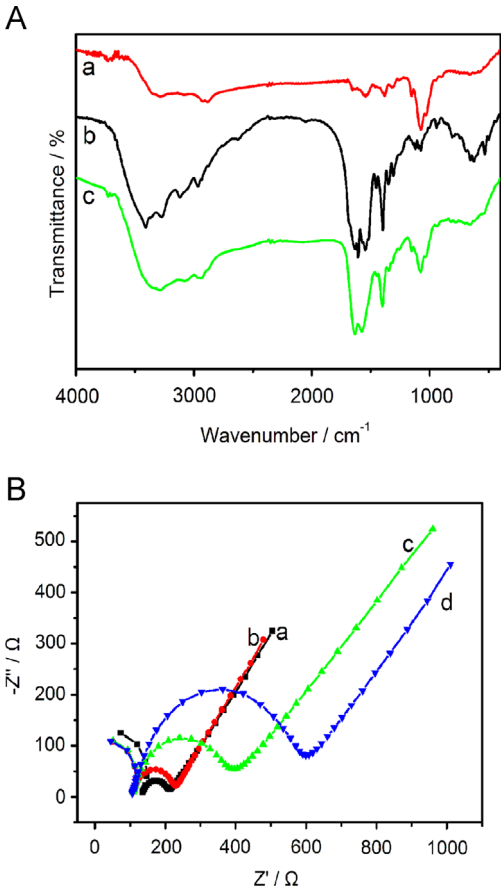

Fig. 2. FTIR spectra of (A) of TCS-TiO_2/chitosan (a), GOx (b) and GOx/TCS-TiO_2/chitosan (c), and Nyquist plots of EIS (B) for bare (a), chitosan (b), TCS-TiO_2/chitosan (c) and GOx/TCS-TiO_2/chitosan (d) modified GCEs.

showed an incompact porous structure, indicating the successful immobilization of enzyme in the TCS-TiO_2/chitosan nanocomposite film.

FTIR spectroscopy, a useful means for studying the structure and conformation of the proteins, here was used to characterize the existing state of the GOx molecules loaded in the TCS-TiO_2 structure. The FTIR spectra of the TCS-TiO_2/chitosan, native GOx and GOx/TCS-TiO_2/chitosan were shown in Fig. 2A. The absorption band at 1075 cm^{-1} of chitosan is characteristic of frame symmetric and asymmetric flexible vibrations, and the peak at 1394 cm^{-1} is assigned to CH_2 bending (curve a). The FTIR spectrum of native GOx exhibited two characteristic peaks at 1634 and 1554 cm^{-1}, which were ascribed to amide I and II bands of enzyme (curve b). As seen from the FTIR spectrum of GOx/TCS-TiO_2/chitosan, two characteristic absorption peaks at 1641 (amide I band) and 1578 (amide II band) cm^{-1} could be also observed, indicating that GOx molecules were successfully immobilized in the TCS-TiO_2/chitosan composite film (Shi et al., 2003). Small shifts were observed from the absorption peaks of the amide I and II bands between native GOx and GOx trapped in TCS-TiO_2/chitosan film, suggesting the molecular interaction between enzyme and the nanocomposite film (Fan et al., 2007).

EIS is a powerful tool to study the interface property of the surface-modified electrode. The Nyquist plots of different electrodes in the frequency range of 0.05 Hz to 10 KHz were shown in Fig. 2B. For the bare GCE, the electron transfer resistance (R_{ct}) was about 70 Ω (curve a). The R_{ct} of the chitosan/GCE (120 Ω, curve b) was larger than that of the bare GCE, demonstrating that a layer of chitosan film was formed on the surface of GCE, and block the electrode transfer between the redox probe ($K_3[Fe(CN)_6]/K_4[Fe(CN)_6]$) and the electrode surface (Kang et al., 2009; Lin et al., 2009). As seen from the curve c, the R_{ct} of the TCS-TiO_2/chitosan modified GCE increased to 300 Ω. After GOx was immobilized in the TCS-TiO_2/chitosan composite, its R_{ct} further increased to 500 Ω. This result indicated that GOx molecules were steadily absorbed into the TCS-TiO_2/chitosan film on the electrode surface, causing a little bit of inhibition of the electron transfer of redox couple (Kang et al., 2009).

3.2. Direct electrochemistry of GOx/TCS-TiO_2/chitosan/GCE

It is well-known that direct electrochemistry between GOx and electrode surface can be observed from the electrochemical response under proper conditions, and has been used to construct electrochemical biosensors (Nadzhafova et al., 2007; Wu et al., 2007; Deng et al., 2008; Yang et al., 2012). Fig. 3 showed the cyclic voltammograms of different modified GCEs in 0.1 M N_2-saturated PBS at a scan rate of 100 mV s^{-1}. As seen from the cyclic voltammogram curve of TCS-TiO_2/chitosan/GCE (curve a), no peaks were observed. However, GOx/chitosan/GCE exhibited a pair of distinct and well-defined redox peaks (curve b). In comparison with GOx/chitosan/GCE, GOx/TCS-TiO_2/chitosan/GCE showed a pair of more distinct and better-defined redox peaks at −0.430 V and −0.484 V (curve c), indicating TCS-TiO_2 can enable more effective electrical contact between redox-active centers of enzyme and electrode surface, and thus facilitate direct electrochemistry of GOx (Willner et al., 2006). The reduction peak current of GOx/TCS-TiO_2/chitosan/GCE is 2.36 times as large as GOx/chitosan/GCE, which may result from the larger specific surface of TCS-TiO_2, leading to a large response (Dai et al., 2009). The peak potential separation was 54 mV, which is much smaller than that of 80 mV at GOx/graphene-chitosan modified GCE (Kang et al., 2009), indicating the faster DET between the redox-active site of GOx (the cofactor FAD) and GCE surface (Deng et al., 2009).

The effect of the scan rate on the redox peaks current at GOx/TCS-TiO_2/chitosan/GCE was investigated in Fig. S1. It could be observed that with the increase of the scan rate, the redox potentials of GOx shifted slightly. At the same time, the anodic current (I_{pa}) and cathodic peak current (I_{pc}) linearly enhanced with the increasing scan rate from 10 to 400 mV s^{-1} (inset a of Fig. S1). The I_{pa}/I_{pc} ratio is approximately equal to 1, indicating that the redox reaction process of GOx at TCS-TiO_2/chitosan/GCE was a quasi-reversible surface-controlled process. The logarithm plot of cathodic peak current versus logarithm of the scan rate showed a linear relationship (inset b of Fig. S1). The linear regression equation was $\lg I_{pc} = 0.851 \lg \nu - 1.71$ ($R^2 = 0.9906$), and the slope

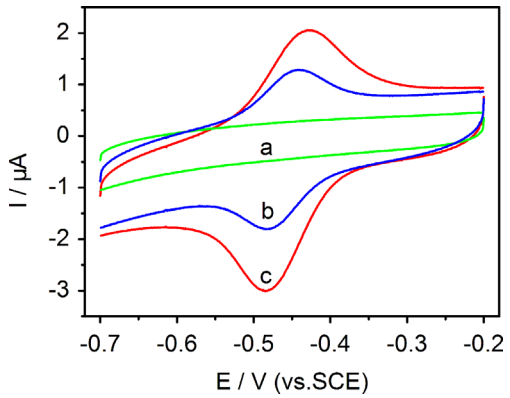

Fig. 3. Cyclic voltammograms of TCS-TiO_2/chitosan/GCE (a), GOx/chitosan/GCE (b), and GOx/TCS-TiO_2/chitosan/GCE (c) in 0.1 M pH 7.0 N_2-saturated PBS at a scan rate of 100 mV s^{-1}.

was very close to the theoretical slope for thin layer electrochemical behavior (Bard and Faulkner, 2001).

The surface coverage (Γ^*) of the enzyme molecules on the surface of the TCS-TiO_2/chitosan modified electrode can be obtained according to the formulation $\Gamma^*=Q/nFA$, where Q is the charge consumed in the reaction, n the number of electrons transferred, F the Faraday constant, and A the electrode area. The surface coverage was calculated to be 3.32×10^{-11} mol cm^{-2} using the charge integration of cathodic peak in cyclic voltammogram at 100 mV s^{-1}, which was larger than those of 1.60×10^{-11} mol cm^{-2} at GOx/SnS_2/Nafion/GCE (Yang et al., 2011), 9.8×10^{-12} mol cm^{-2} at GOx/Au nanoparticles/carbon paste electrode (Liu and Ju, 2003), 7.82×10^{-12} mol cm^{-2} at GOx/Au-dihexadecyl phosphate modified electrode (Wu and Hu, 2007) and 2.86×10^{-12} mol cm^{-2} at bare GCE (Zhang et al., 2007). The large surface coverage may be ascribed to the rod arrays structure of TCS-TiO_2 material, thus leading to larger surface area of the modified electrode.

The influence of the pH value on the electrochemical behavior of GOx/TCS-TiO_2/chitosan/GCE was examined. As shown in Fig. S2, both the cathodic and anodic peak potentials shifted negatively with the increase of the solution pH values. The redox potentials of GOx/TCS-TiO_2/chitosan/GCE changed linearly as a function of the solution pH from 4.0 to 8.0 with a slope of -50.0 mV pH^{-1} ($R^2=0.9976$, inset a of Fig. S2). This slope was close to the theoretical value of -58.6 mV pH^{-1} reported previously (Deng et al., 2009), indicating same proton and same electron attending in the electron transfer process. In addition, the redox peaks current reached its maximum value at pH 7.0 (inset b of Fig. S2), suggesting the optimal solution pH for the immobilization of GOx. Because the proton participates in the redox process of GOx, the decrease of GOx response at higher pH value may be attributed to the decrease of proton concentration, while the decreased peak current at lower pH value is possible due to decreased bioactivity of immobilized GOx (Wen et al., 2007; Yang et al., 2009).

3.3. Performance of the proposed glucose biosensor

Fig. 4 showed the cyclic voltammograms of TCS-TiO_2/chitosan/GCE and GOx/TCS-TiO_2/chitosan/GCE in nitrogen- and air-saturated pH 7.0 PBS in the absence and presence of glucose. In air-saturated PBS, no peak was observed at TCS-TiO_2/chitosan/GCE (curve b in Fig. 4A), though an increase in reduction current at potentials more negative than -0.4 V. However, a great increase in reduction peak current and a simultaneous decrease in oxidation current could be clearly observed from a cyclic voltammogram of GOx/TCS-TiO_2/chitosan/GCE (curve e in Fig. 4B), indicating a typical electrocatalytic process. GOx ($FADH_2$) species reacted with dissolved O_2 and generated GOx (FAD) that could be reduced on GCE surface according to the following equations (Liu and Ju, 2003).

$$\text{GOx (FAD)}+2e^-+2H^+\leftrightarrow\text{GOx (}FADH_2\text{)} \quad (1)$$

$$\text{GOx (}FADH_2\text{)}+O_2\rightarrow\text{GOx (FAD)}+H_2O_2 \quad (2)$$

When glucose was added into this system, it restrained the electrocatalytic reaction due to the enzyme-catalyzed reaction, which reduced the concentration of GOx (FAD) as shown in the following Eq. (3). Therefore, the reduction peak current of GOx/TCS-TiO_2/chitosan/GCE decreased (curve f in Fig. 4B). However for TCS-TiO_2/chitosan/GCE, no obvious change was observed upon addition of glucose to air-saturated PBS (curve c in Fig. 4A). Based on the response of GOx/TCS-TiO_2/chitosan/GCE to glucose, an enzyme biosensor was therefore proposed for sensitive detection of glucose in this work.

$$\text{Glucose}+\text{GOx (FAD)}+O_2\rightarrow\text{Gluconolactone}+\text{GOx (}FADH_2\text{)} \quad (3)$$

Fig. 5A showed the cyclic voltammograms of GOx/TCS-TiO_2/chitosan/GCE in pH 7.0 air-saturated PBS containing different concentrations of glucose. With the increase of glucose concentrations, the reduction current response decreased correspondingly. Fig. 5B displayed the typical amperometric response curve at GOx/TCS-TiO_2/chitosan modified GCE on successive injection of glucose to the air-saturated stirring PBS (the optimal pH value and applied potential for the amperometric detection of glucose were chosen as pH 7.0 and -0.5 V). The GOx/TCS-TiO_2/chitosan/GCE achieved 95% of the steady-state current only within 3 s. The current response increased linearly with the increase of glucose concentration ranging from 5.0×10^{-6} to 1.32×10^{-3} M with a high sensitivity of 23.2 mA M^{-1} cm^{-2} and a correlation coefficient of 0.9992 (Inset of Fig. 5B). The detection limit for glucose at GOx/TCS-TiO_2/chitosan/GCE was calculated to be of 2.0×10^{-6} M at signal-to-noise of 3. The analytical performance of this work was compared to that of the literatures reported recently for the glucose biosensor in Table 1. In comparison with other types of enzyme electrodes, the proposed GOx/TCS-TiO_2/chitosan/GCE showed obvious predominance such as obviously higher sensitivity and lower detection limit.

The apparent Michaelis–Menten constant (K_M^{app}) is an indicator of enzyme–substrate reaction kinetics, and can be used to evaluate

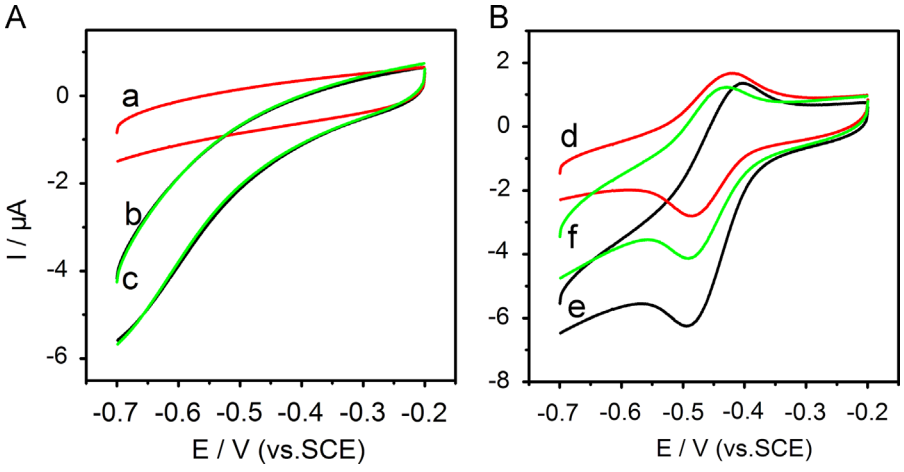

Fig. 4. Cyclic voltammograms of TCS-TiO_2/chitosan/GCE (A) and GOx/TCS-TiO_2/chitosan/GCE (B) in 0.1 M pH 7.0 N_2-saturated PBS (a and d), air-saturated PBS (b and e), air-saturated PBS including 0.5 mM glucose (c and f) at a scan rate of 100 mV s^{-1}.

the bioactivity of the immobilized enzyme. K_M^{app} for the glucose biosensor was calculated to be 0.41 mM according to the Lineweaver–Burk equation: $1/I_{ss} = (1/I_{max}) + (K_M^{app}/I_{max})(1/C)$ (Scott and Bowden, 1994). Here, I_{ss} is the steady-state current after the addition of substrate, C is the bulk concentration of substrate and I_{max} is the maximum current measured at the saturated substrate solution. The K_M^{app} value was much smaller than those of 4.4, 11.6, 37.6 and 18.94 mM for immobilized GOx (Zheng et al., 2002; Uang and Chou, 2003; Kang et al., 2009, Cai et al., 2012), indicating that the GOx immobilized in TCS-TiO_2/chitosan has high affinity towards glucose.

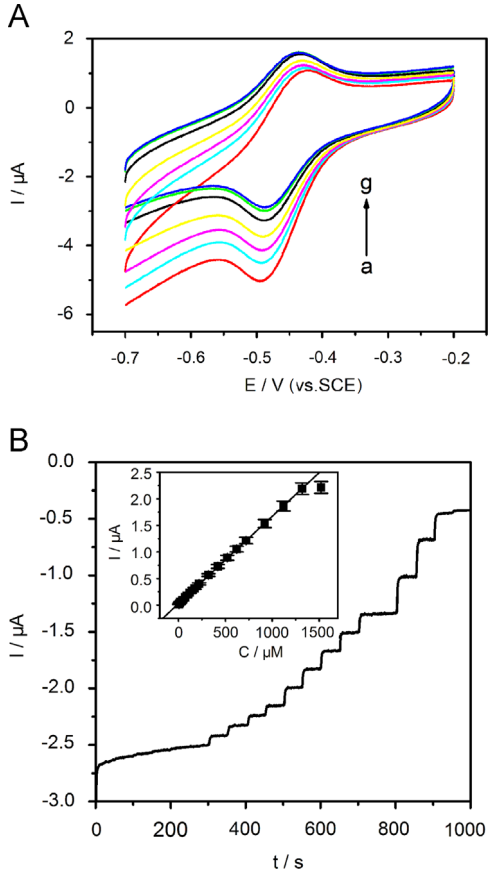

Fig. 5. Cyclic voltammograms of GOx/TCS-TiO_2/chitosan /GCE (A) in 0.1 M pH 7.0 air-saturated PBS including 0.1, 0.3, 0.5, 0.7, 1.0, 1.5 and 2.0 mM glucose (a–g) at a scan rate of 100 mV s^{-1}, and typical steady-state response of GOx/TCS-TiO_2/chitosan/GCE (B) on successive addition of glucose into 0.1 M pH 7.0 air-saturated PBS at the applied potential of −0.50 V, inset: calibration curve of GOx/TCS-TiO_2/chitosan/GCE for glucose.

3.4. Reproducibility and stability of the glucose biosensor

The reproducibility of the proposed biosensor was investigated by detecting 0.1 mM glucose for 5 times at the same enzyme electrode, the relative standard deviation (RSD) was 3.8%, indicating a good detection reproducibility. After 20 successive detections, the response still retained 95% of the initial value, suggesting the acceptable operational stability. The reproducibility of the enzyme electrode was also examined by measuring 0.1 mM glucose at 5 different modified electrodes, and the RSD was 5.4%, indicating good fabrication reproducibility. The enzyme electrode was stored at 4 °C when not in use. It can retained 96% of its initial current response after storage for three weeks, demonstrating that the TCS-TiO_2/chitosan composite provided a favorable microenvironment to retain acceptable long-term life time of the glucose biosensor.

3.5. Interference study and detection of glucose in the practical serum samples

Fig. S3 showed the interferences in quantitative detection of glucose using 0.1 mM uric acid (UA) and 0.1 mM ascorbic acid (AA) at the applied potential of −0.50 V. Upon the addition of 0.1 mM glucose to pH 7.0 PBS, a clear current response could be observed. When the AA and UA were successively injected into the solution, there was no obvious increase of the current. After addition of 0.1 mM glucose to the system again, the amperometric response was almost close to the value detected in absence of the interferents, suggesting the excellent selectivity of the proposed glucose biosensor toward glucose.

The practical samples were measured to evaluate the potential application of the constructed glucose biosensor. The human serum samples were received from Northern Jiangsu People's Hospital without any sample pretreatment except a dilution step. The glucose level was determined to be 5.54 mM, which is close to the value of 5.70 mM obtained by enzyme catalytic spectrophotometry. The recoveries for the assay of 0.05 and 0.1 mM glucose added in the serum samples were 103% with a RSD of 1.2% and 100% with a RSD of 1.9% for five measurements, showing good accuracy of the biosensor in the detection of the real samples.

4. Conclusions

Here, a novel tetragonal columnar-shaped TiO_2 nanorods were synthesized by heating the mixture of Ti and NH_4Cl powders in air at 400 °C. The method is simple, low temperature and low cost. The TCS-TiO_2 was for the first time used to modify electrode for the immobilization of enzyme and construction of sensitive glucose biosensor. Scanning electron microscopy, Fourier transform infrared

Table 1
Comparison of analytical performance between GOx/TCS-TiO_2/chitosan/GCE and other modified electrodes.

Electrode	Applied potential (V)	Sensitivity (mA M^{-1} cm^{-2})	Detection limit (mM)	Linear range (mM)	Reference
GOx/TCS-TiO_2/chitosan/GCE	−0.50	23.2	0.002	0.005–1.32	This work
GOx/TiO_2-graphene/GCE	−0.60	6.2	–	0.0–8.0	Jiang et al. (2012a)
GOx/SnS_2/Nafion/GCE	−0.45	7.6	0.01	0.025–1.1	Yang et al. (2011)
GOx/TPSP-ZnO/Nafion/GCE	−0.50	–	0.01	0.05–8.2	Dai et al. (2009)
GOx/CNx-MWNTs/GCE	−0.50	13.0	0.01	0.02–1.02	Deng et al. (2009)
Nafion/GOx/Ag-Pdop@CNT/GCE	−0.50	3.1	0.017	0.05–1.1	Wang et al. (2011)
Laponite/GOx/GCE	−0.45	4.8	0.01	0.02–1.9	Shan et al. (2010a, 2010b)
GOx/Pt/FCNA/GCE	−0.08	6.0	0.3	0.5–8.0	Tang et al. (2010)

TPSP: tetragonal pyramid-shaped porous.
CNx-MWNTs: nitrogen-doped carbon nanotubes.
Pdop: polydopamine.
FCNA: flower-like carbon nanosheet aggregation.

spectroscopy, electrochemical impedance spectra and cyclic voltammetry were used to characterize the fabricated biosensor. The larger specific surface area of TCS-TiO_2 provides a favorable microenvironment for retaining its bioactivity of the immobilized enzyme and enhances the electron transfer between enzyme and the electrode surface. The glucose biosensor exhibits fast amperometric response, excellent selectivity and good reproducibility. The excellent performances such as high sensitivity (23.2 mA M^{-1} cm^{-2}), low detection limit (0.002 mM) and wide linear range (0.005–1.32 mM) were obtained at the proposed biosensor. The satisfactory results of the serum samples measured at the enzyme electrode shows the practical application of the biosensor. In brief, this work provides a promising TCS-TiO_2 matrix for immobilizing proteins and developing novel biosensors.

Acknowledgments

This work was financially supported by National Natural Science Foundation of China (21075107, 21005070 and 21103148), The Priority Academic Program Development of Jiangsu Higher Education Institution (PAPD), Postdoctoral Science Foundation of China (20110491462, 2012T50519) and University Natural Science Foundation of Jiangsu Province (13KJB150039).

Appendix A. Supplementary material

Supplementary data associated with this article can be found in the online version at http://dx.doi.org/10.1016/j.bios.2013.11.043.

References

Ammam, M., Fransaer, J., 2012. Biotechnol. Bioeng. 109, 1601–1609.
Attar, A.S., Ghamsari, M.S., Hajiesmaeilbaigi, F., Mirdamdi, S., Katagiri, K., Koumoto, K., 2009. Mater. Chem. Phys. 113, 856–860.
Azamian, B.R., Davis, J.J., Coleman, K.S., Bagshaw, C.B., Green, M.L.H., 2002. J. Am. Chem. Soc. 124, 12664–12665.
Bao, S.J., Li, C., Zang, J.F., Cui, X.Q., Qiao, Y., Guo, J., 2008. Adv. Funct. Mater. 18, 591–599.
Bard, J., Faulkner, L.R., 2001. Electrochemistry Methods, 2nd ed. Wiley, New York.
Cai, C.J., Xu, M.W., Bao, S.J., Lei, C., Jia, D.Z., 2012. RSC Adv., 8172–8178.
Chung, Y.A., Lee, C.Y., Peng, C.W., Chiu, H.T., 2006. Mater. Chem. Phys. 100, 380–384.
Dai, Z.H., Shao, G.J., Hong, J.M., Bao, J.C., Shen, J., 2009. Biosens. Bioelectron. 24, 1286–1291.
Deng, C.Y., Chen, J.H., Chen, X.L., Xiao, C.H., Nie, L.H., Yao, S.Z., 2008. Biosens. Bioelectron. 23, 1272–1277.
Deng, S.Y., Jian, G.Q., Lei, J.P., Hu, Z., Ju, H.X., 2009. Biosens. Bioelectron. 25, 373–377.
Fan, Q., Shan, D., Xue, H.G., He, Y.Y., Cosnier, S., 2007. Biosens. Bioelectron. 22, 816–821.
Jia, F., Shan, C.S., Li, F.H., Niu, L., 2008. Biosens. Bioelectron. 24, 945–950.
Jiang, H.D., Kim, S.K., Chang, H.K., Roh, K.M., Choi, J.W., Huang, J., 2012a. Biosens. Bioelectron. 38, 184–188.
Jiang, Y.Y., Zhang, Q.X., Li, F.H., Niu, L., 2012b. Sens. Actuators B 55, 728–733.
Kang, X.H., Wang, J., Wu, H., Aksay, I.A., Liu, J., Lin, Y.H., 2009. Biosens. Bioelectron. 25, 901–905.
Koo, B., Park, J., Kim, Y., Choi, S.H., Sung, Y.E., Hyeon, T., 2006. J. Phys. Chem. B 110, 24318–24323.
Li, J., Yang, Z.J., Tang, Y., Zhang, Y.C., Hu, X.Y., 2013. Biosens. Bioelectron. 41, 698–703.
Liang, H.T., Li, X.Z., 2009. J. Hazard. Mater. 162, 1415–1422.
Lin, J.H., He, C.Y., Zhao, Y., Zhang, S.S., 2009. Sens. Actuators B 137, 768–773.
Liu, S.Q., Ju, H.X., 2003. Biosens. Bioelectron. 19, 177–183.
Meng, L., Jin, J., Yang, G.X., Lu, T.H., Zhang, H., Cai, C.X., 2009. Anal. Chem. 81, 7271–7280.
Mizutani, F., Yabuki, S., 1997. Biosens. Bioelectron. 12, 1013–1020.
Nadzhafova, O., Etienne, M., Walcarius, A., 2007. Electrochem. Commun. 9, 1189–1195.
Pingarron, J.M., Yanez-Sedeno, P., Gonzalez-Cortes, A., 2008. Electrochim. Acta 53, 5848–5866.
Shan, C.S., Yang, H.F., Han, D.X., Zhang, Q., Ivaska, A., Niu, L., 2010a. Biosens. Bioelectron. 25, 1070–1074.
Shan, D., Zhang, J., Xue, H.G., Ding, S.N., Cosnier, S., 2010b. Biosens. Bioelectron. 25, 1427–1433.
Shi, C., Liu, Q., Xie, Y., Xu, X., 2003. J. Mol. Struct. 644, 139–144.
Scott, D.L., Bowden, E.F., 1994. Anal. Chem. 66, 1217–1223.
Tang, S., Wang, X.Z., Lei, J.P., Hu, Z., Deng, S.Y., Ju, H.X., 2010. Biosens. Bioelectron. 26, 432–436.
Tian, G., Fu, H., Jing, L., Xin, B., Pan, K., 2008. J. Phys. Chem. C 112, 3083–3089.
Uang, Y., Chou, T.C., 2003. Biosens. Bioelectron. 20, 2435–2453.
Vamvakai, V., Tsagaraki, K., Chaniotakis, N., 2006. Anal. Chem. 78, 5538–5542.
Wang, J., 2008. Chem. Rev. 108, 814–825.
Wang, J., Musameh, M., 2003. Anal. Chem. 75, 2075–2079.
Wang, Y.L., Liu, L., Li, M.G., Xu, S.D., Gao, F., 2011. Biosens. Bioelectron. 30, 107–111.
Wang, Z.Y., Xia, D.G., Chen, G., Yang, T., Chen, Y., 2008. Mater. Chem. Phys. 111, 313–316.
Wen, D., Liu, Y., Yang, G.C., Dong, S.J., 2007. Electrochim. Acta 52, 5312–5317.
Willner, B., Katz, E., Willner, I., 2006. Curr. Opin. Biotechnol. 17, 589–596.
Wu, S., Ju, X.H., Liu, Y., 2007. Adv. Funct. Mater. 17, 585–592.
Wu, Y.H., Hu, S.S., 2007. Bioelectrochemistry 70, 335–341.
Xu, X.A., Jiang, S.J., Hu, Z., Liu, S.Q., 2010. ACS Nano 4, 4292–4298.
Yang, L.Q., Ren, X.L., Tang, F.Q., Zhang, L., 2009. Biosens. Bioelectron. 25, 889–895.
Yang, Z.J., Ren, Y.Y., Zhang, Y.C., Li, J., Li, H.B., Huang, X.C., Hu, X.Y., Xu, Q., 2011. Biosens. Bioelectron. 26, 4337–4341.
Yang, Z.J., Huang, X.C., Zhang, Y.C., Li, Juan, Xu, Q., Hu, X.Y., 2012. Electrochim. Acta 70, 325–330.
Zhang, J.D., Feng, M.L., Tachikawa, H., 2007. Biosens. Bioelectron. 22, 3036–3041.
Zhang, S., Liu, C.Y., Liu, Y., Zhang, Z.Y., Mao, L.J., 2009. Mater. Lett. 63, 127–129.
Zhao, H.T., Ju, H.X., 2006. Anal. Biochem. 350, 138–144.
Zheng, H., Xue, H., Zhang, Y., Shen, Z., 2002. Biosens. Bioelectron. 17, 541–545.